Tectonophysics 712-713 (2017) 193–199

Contents lists available at ScienceDirect

Tectonophysics

journal homepage: www.elsevier.com/locate/tecto

Lateral variations of crustal structure beneath the Indochina Peninsula

Youqiang Yu[a,*], Tran D. Hung[a,b], Ting Yang[c], Mei Xue[a], Kelly H. Liu[d], Stephen S. Gao[d]

[a] State Key Laboratory of Marine Geology, Tongji University, Shanghai 200092, China
[b] Department of Geophysics, Hanoi University of Mining and Geology, Hanoi 100000, Vietnam
[c] School of Oceanography, Southern University of Science and Technology (SUSTech), Shenzhen, Guangdong 518055, China
[d] Geology and Geophysics Program, Missouri University of Science and Technology, Rolla, MO 65409, USA

ARTICLE INFO

Article history:
Received 15 February 2017
Received in revised form 20 May 2017
Accepted 26 May 2017
Available online 29 May 2017

Keywords:
Crustal structure
Indochina Peninsula
Receiver function
Extrusion

ABSTRACT

Crustal thickness (H) and V_p/V_s (κ) measurements obtained by stacking P-to-S receiver functions recorded at 32 broadband seismic stations covering the Indochina Peninsula reveal systematic spatial variations in crustal properties. Mafic bulk crustal composition as indicated by high κ (>1.81) observations is found to exist along major strike-slip faults and the southern part of the Peninsula, where pervasive basaltic magmatism is found and is believed to be the results of lithospheric thinning associated with the indentation of the Indian into the Eurasian plates. In contrast, crust beneath the Khorat Plateau, which occupies the core of the Indochina Block, has relatively large H values with a mean of 36.9 ± 3 km and small κ measurements with an average of 1.74 ± 0.04, which indicates an overall felsic bulk composition. Those observations for the Khorat Plateau are comparable to the undeformed part of the South China Block. The laterally heterogeneous distribution of crustal properties and its correspondence with indentation-related tectonic features suggest that the Indochina lithosphere is extruded as rigid blocks rather than as a viscous flow.

1. Introduction

The indentation of the rigid Indian plate into the Eurasian plate has resulted in significant tectonic deformation in the Asian continent since the Eocene (e.g., Tapponnier et al., 1982; Huchon et al., 1994; Chi and Geissman, 2013). The collision not only generated the world's highest mountain system and plateau, but also led to the development of major strike-slip faults and lateral extrusion of continental blocks towards the east and southeast (e.g., Achache et al., 1983; Richter and Fuller, 1996; Charusiri et al., 2006; Morley, 2012; Chi and Geissman, 2013; Tsuchiyama et al., 2016). The Indochina Peninsula (Fig. 1), which is situated immediately to the southeast of the eastern Himalayan syntaxis, has been extruded by about 700 km along the Red River Fault (e.g., Tapponnier et al., 1982; Leloup et al., 1995; Searle, 2006; Wen et al., 2015), and thus is an ideal locale to investigate the impact of extrusion tectonics on crustal deformation (Fig. 1).

The Indochina Peninsula is mainly composed of the Shan-Thai Block on the north and the Indochina Block on the south, and is surrounded by strike-slip faults with the Red River Fault to the northeast, Sagaing Fault to the northwest, and the Wang Chao and Three Pagodas faults to the southwest (Fig. 1; Sato et al., 2007; Takemoto, 2009; Morley, 2012). Paleomagnetic studies revealed that the Indochina Peninsula has suffered from a clock-wise rotation coupled with southward displacement relative to the South China Block since the Cretaceous (e.g., Achache et al., 1983; Sato et al., 2001; Takemoto, 2009; Morley, 2012). The Red River Fault, which separates the Indochina and Shan-Thai Blocks from the South China Block, is closely associated with the opening of the South China Sea (Briais et al., 1993; Yang and Besse, 1993; Leloup et al., 1995; Chung et al., 1997; Searle, 2006; Yang et al., 2015). The present-day boundary between the Shan-Thai and Indochina blocks is possibly defined by the ancient Nan-Uttaradit suture zone, and the Triassic Song Ma Suture may accommodate the lateral deformation resulted from the relative motion between the Indochina and South China Blocks (Yang and Besse, 1993; Wen et al., 2015). The Indochina Block is mainly occupied by the Khorat Plateau within which the Khorat Basin developed (Fig. 1), and is covered by Mesozoic continental red beds (Otofuji et al., 2012).

A number of models have been proposed to explain the deformation mechanisms of the Indochina Peninsula, and the two most-cited ones are the crustal extrusion model and the viscous flow model (e.g., England and Houseman, 1986; Yang et al., 2015). The former advocates that the deformation is localized along the faults where the entire lithosphere slides as rigid blocks; in contrast, the viscous flow model suggests that strain induced by the collision is accommodated

* Corresponding author.
E-mail address: yuyouqiang@tongji.edu.cn (Y. Yu).

http://dx.doi.org/10.1016/j.tecto.2017.05.023
0040-1951/

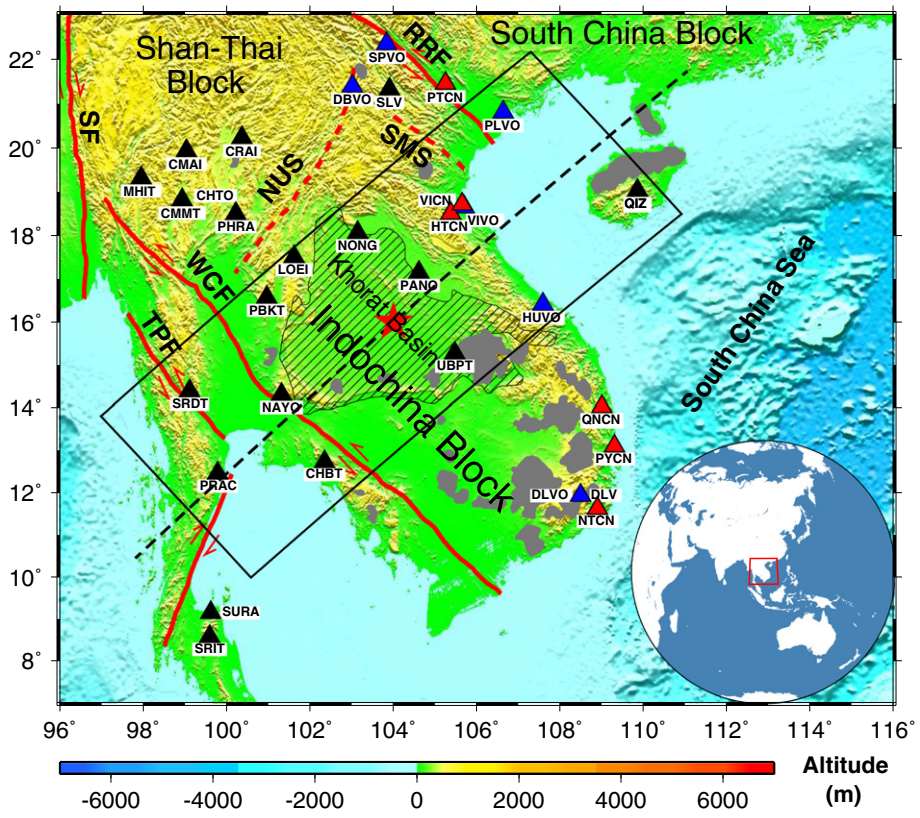

Fig. 1. Topographic map of the Indochina Peninsula showing the distribution of seismic stations (triangles) used in the study and major tectonic features. Black triangles represent IRIS stations, red triangles indicate stations deployed by Tongji University, and blue triangles show stations belonging to the University of Tokyo. Red solid and dashed lines represent major faults and sutures, respectively, modified from Leloup et al. (1995) and Takemoto (2009). Areas filled with slashed lines indicate the Khorat Basin. Gray shaded areas indicate Cenozoic volcanic centers modified from Hoang and Flower (1998) and Fedorov and Koloskov (2005). Data from stations within the black rectangle are used to plot the cross section in Fig. 3 along the dashed black line where the point of the zero distance is marked as a red star. NUS: Nan-Uttradit Suture; RRF: Red River Fault; SF: Sagaing Fault; SMS: Song Ma Suture; TPF: Three Pagodas Fault; WCF: Wang Chao Fault. The red rectangle in the inset map shows the location of the study area. (For interpretation of the references to color in this figure legend, the reader is referred to the web version of this article.)

by approximately homogeneous thickening of the crust (England and Houseman, 1986; Tapponnier et al., 1982). Therefore, spatial distribution of crustal properties such as thickness (H) and V_p/V_s (κ), which is uniquely related to the Poisson's ratio and is mostly dependent on crustal composition, can provide important constraints on models of crustal deformation under extrusion tectonics.

In this study, we utilize the receiver function (RF) technique (Langston, 1979; Ammon, 1991; Zhu and Kanamori, 2000) to characterize crustal properties beneath the Indochina Peninsula. Previous RF studies were conducted in relatively localized areas, including Thailand (Tadapansawut et al., 2012; Noisagool et al., 2014), northern Vietnam (Nguyen et al., 2013), and beneath a network of sparsely-distributed stations in Vietnam (Bai et al., 2010). A variety of data processing approaches and parameters were used in these studies, resulting in a heterogeneous data set. Additionally, the limited spatial coverage of previous studies prevents a comprehensive understanding of crustal structure and composition under various tectonic settings. Here we present results from a teleseismic RF study of the entire Indochina Peninsula by utilizing all the available seismic datasets and systematically investigate the role of extrusion tectonics played on the modification of crustal properties in different tectonic domains.

2. Data and methods

Broadband seismic data used in this study were recorded by a total of 32 stations belonging to three networks (Table 1), including 6 stations deployed by the Seismological Group at Tongji University along the coast of Vietnam during a three year period starting from 2009 (Yang et al., 2015), 6 stations in the Vietnam broadband seismograph array for the period of February 2000 to October 2005 (Bai et al., 2009, 2010), and 20 stations throughout the study area with data publicly available at the Incorporated Research Institutions for Seismology (IRIS) Data Management Center (DMC).

Data from teleseismic events with epicentral distances greater than 30° were selected. The cutoff magnitude was defined as $M_c = 5.2 + (D_e - 30.0)/(180.0 - 30.0) - H_f/700.0$, where D_e and H_f are the epicentral distance in degrees and the focal depth in kilometers, respectively. Such a formula aims to take advantage of high-quality waveforms from deep earthquakes, reaching an optimal balance between quantity and quality of seismic data utilized (Liu and Gao, 2010). The three component seismograms are windowed to 20 s prior to and 260 s after the first P-wave arrival based on the IASP91 Earth model, and are band-pass filtered using a 4 pole, 2 pass Butterworth filter with corner frequencies of 0.08 and 0.8 Hz. The filtered seismograms with a P-wave signal to noise ratio of 4.0 or greater on the radial component were selected to generate radial RFs utilizing the frequency domain water level deconvolution procedure of Ammon (1991). A water level of 0.03 was adopted to stabilize the deconvolution.

To identify and correct for possible sensor misorientation, we applied the technique proposed by Niu and Li (2011), which is based on the minimization of the P-wave energy on the transverse component. High-quality seismograms with a robust first arrival of the

direct *P*-phase on the vertical component were selected by manual picking, and then go through a grid-search stacking procedure to determine the optimal orientation of the N-S component for each station, which corresponds to the minimum *P*-wave energy on the transverse components. Subsequently, the resulting optimal orientation for each station was used to correct the N-S and E-W seismograms.

The orientation-corrected seismograms were converted into radial RFs, and were visually checked to reject those without well-defined first *P* arrivals. We then employed the *H*-κ stacking procedure to moveout correct and stack the selected RFs to determine the optimal crustal *H* and κ for each station (Zhu and Kanamori, 2000). In this study, an average crustal *P*-wave velocity of 6.3 km/s was chosen based on previous RF studies in the Indochina Peninsula (Bai et al., 2010; Noisagool et al., 2014). A series of combinations of candidate *H* (in the range of 15–55 km with an interval of 0.1 km) and κ (1.65 to 1.95 with a step of 0.01) were employed in a weighted phase-specific stacking procedure (Zhu and Kanamori, 2000) and the optimal pair of crustal *H* and κ corresponds to the maximum stacking amplitude on the *H*-κ plot (Fig. 2). We applied the bootstrap resampling approach (Efron and Tibshirani, 1986) with 10 iterations to calculate the mean and standard deviation of the optimal pair of *H* and κ for each station.

Station UBPT is situated inside the Khorat Basin and suffers from strong reverberations caused by the sedimentary layer. We employed a recently-developed reverberation-removal technique to reduce the delay effects from the underlain sediment and more realistically determine crustal *H* and κ based on an updated *H*-κ stacking procedure (Yu et al., 2015a). Such a technique has been recently applied to the Okavango rift zone (Yu et al., 2015b).

To demonstrate the quality of the RF traces, we migrated the RFs of representative stations across the Indochina Peninsula along a profile (Fig. 1). The RFs were converted into depth series using the resulting κ value for each station from *H*-κ stacking. Prominent high-amplitude peaks corresponding to the *P*-to-*S* converted arrivals from the Moho were revealed within the depth window of 10–50 km in the resulting migrated image (Fig. 3), and correlated well with the resulting *H* of *H*-κ stacking for each of the stations.

3. Results

3.1. Sensor orientation correction

Most of the optimal orientations for the N-S component of the 32 sensors fell in the range of $-17^\circ \sim 24^\circ$ clockwise from the north with a simple mean of $4.8^\circ \pm 9.5^\circ$ (Table 1). Among the 32 stations used in this study, significant misorientation or sensor malfunctioning was found for stations DLVO, PANO, and PHRA. The E-W component of station PANO was malfunction during most of the recording time. The same problem happened to station DLVO while the difference is that the E-W component failed to function after middle 2003. Thus,

Table 1
Observations of *H* and *k* for the 32 stations.

Station	Lat.(°)	Lon. (°)	Orient. (°)	*H* (km)	H^a (km)	H^b (km)	*k*	k^a	k^b	N
IRIS										
CHBT	12.744	102.353	−11	39.2 ± 0.0	28.9 ± 0.9		1.77 ± 0.00	1.76 ± 0.02		197
CHTO	18.814	98.944	2	31.8 ± 0.1	32.6 ± 0.5	30.9	1.66 ± 0.01	1.65 ± 0.02	1.65	4774
CMAI	19.933	99.045	0	30.9 ± 0.1	32.2 ± 0.4		1.79 ± 0.01	1.74 ± 0.01		196
CMMT	18.814	98.944	2	31.9 ± 0.2	32.3 ± 0.3		1.66 ± 0.01	1.67 ± 0.01		982
CRAI	20.229	100.373	2	29.4 ± 0.0			1.79 ± 0.00			227
DLV	11.952	108.481	2	34.4 ± 0.0			1.80 ± 0.00			621
LOEI	17.509	101.624	24	33.7 ± 0.1	34.9 ± 1.2		1.78 ± 0.01	1.74 ± 0.01		170
MHIT	19.315	97.963	6	32.4 ± 0.1	34.6 ± 0.2		1.75 ± 0.01	1.67 ± 0.01		292
NAYO	14.315	101.321	4	33.9 ± 0.2	35.2 ± 1.7		1.76 ± 0.01	1.70 ± 0.04		158
NONG	18.063	103.146	11	37.5 ± 0.2	39.3 ± 0.4		1.77 ± 0.01	1.71 ± 0.01		325
PANO	17.148	104.612	–	40.7 ± 0.2			1.70 ± 0.01			59
PBKT	16.573	100.969	4	38.6 ± 0.0	40.0 ± 0.2		1.70 ± 0.00	1.67 ± 0.01		454
PHRA	18.499	100.229	−150/10[d]	32.2 ± 0.0			1.75 ± 0.01			207
PRAC	12.473	99.793	13	28.9 ± 0.2	30.0 ± 0.5		1.69 ± 0.01	1.66 ± 0.01		164
QIZ	19.029	109.843	1	30.9 ± 0.2		31.3	1.79 ± 0.01		1.70	1475
SLV	21.325	103.907	7	30.7 ± 0.0			1.87 ± 0.00			587
SRDT	14.395	99.121	3	29.1 ± 0.1	29.7 ± 0.5		1.74 ± 0.00	1.68 ± 0.02		603
SRIT	8.595	99.602	−17	31.7 ± 0.2			1.68 ± 0.01			68
SURA	9.166	99.629	13	27.1 ± 0.3			1.91 ± 0.02			51
UBPT[c]	15.277	105.469	24	31.9 ± 0.2	33.7 ± 2.8		1.85 ± 0.01	1.79 ± 0.06		225
The University of Tokyo										
DBVO	21.390	103.018	3	33.4 ± 0.1		32.9	1.73 ± 0.00		1.68	217
DLVO	11.945	108.482	1	34.4 ± 0.2		33.9	1.80 ± 0.01		1.79	133
HUVO	16.411	107.580	2	29.0 ± 0.2		30.3	1.74 ± 0.01		1.65	244
PLVO	20.805	106.628	−5	30.6 ± 0.2		29.1	1.73 ± 0.01		1.72	134
SPVO	22.338	103.835	−5	36.6 ± 0.2		34.6	1.79 ± 0.00		1.81	190
VIVO	18.650	105.696	10	28.9 ± 0.2		29.0	1.67 ± 0.01		1.59	255
Tongji University										
HTCN	18.505	105.372	15	28.2 ± 0.1			1.71 ± 0.01			113
NTCN	11.640	108.885	0	31.1 ± 0.5			1.84 ± 0.01			52
PTCN	21.453	105.248	0	31.9 ± 0.1			1.79 ± 0.00			404
PYCN	13.111	109.293	−1	27.3 ± 0.3			1.88 ± 0.02			66
QNCN	14.033	108.991	−6	28.5 ± 0.1			1.80 ± 0.01			260
VICN	18.714	105.646	21	29.2 ± 0.3			1.65 ± 0.01			37

[a] RFs results from Noisagool et al. (2014).
[b] RFs results from Bai et al. (2010).
[c] After applying the reverberation-removal technique.
[d] −150 is for years of 2009–2014 while 10 is for 2015 and 2016.

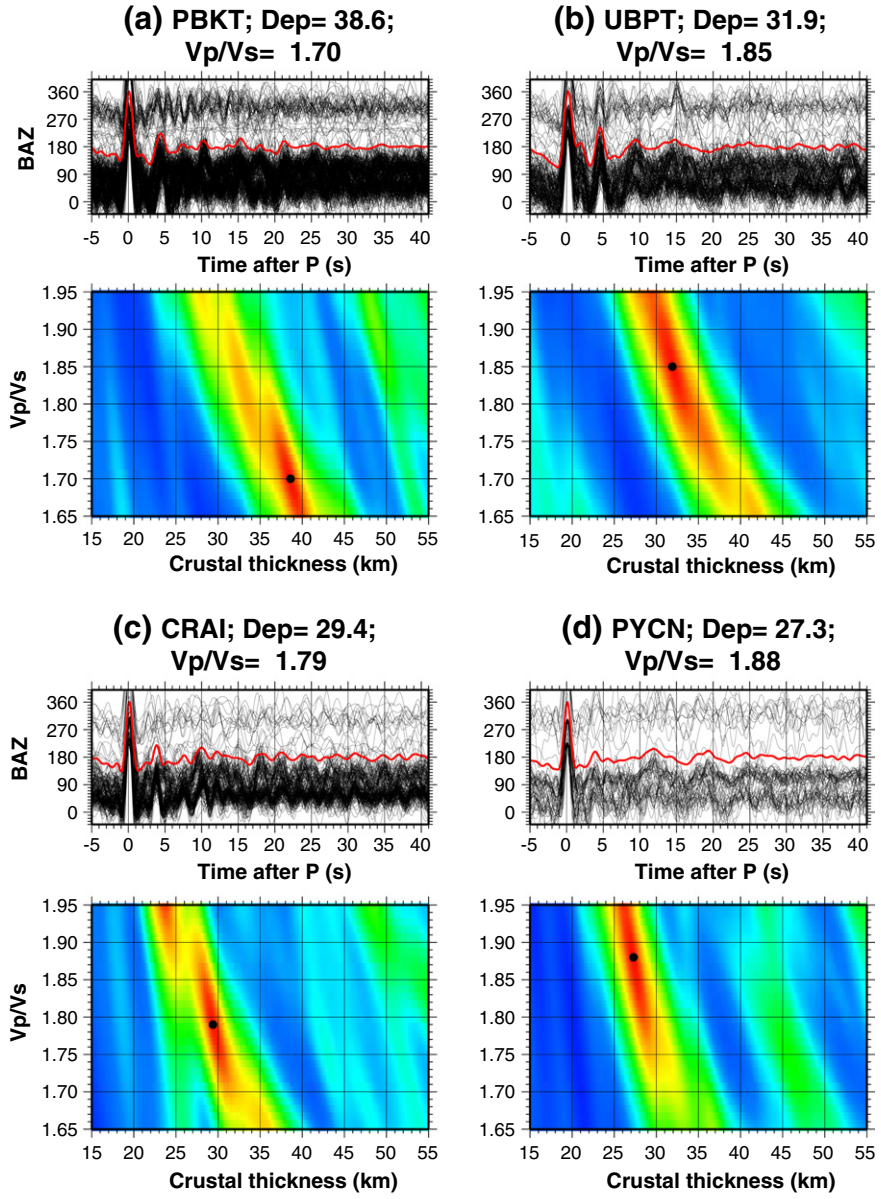

Fig. 2. H-κ stacking results from representative stations of PBKT, UBPT, CRAI and PYCN. The upper panel shows individual receiver functions (black) plotted against back azimuth. The red trace indicates a simple time-domain stack of all the RFs recorded at the station. The lower panel is the H-κ stacking plot with the black dot representing the optimal crustal thickness and V_p/V_s. (For interpretation of the references to color in this figure legend, the reader is referred to the web version of this article.)

we preferred not to calculate the orientation of station PANO and the resulting optimal orientation of station DLVO was determined using data before mid 2003. In spite of the failure of one of the two horizontal components, the RFs were still useful, although the amplitude of the *P*-to-*S* converted waves was lowered and was a function of the back-azimuth of the events. We also found that from 2009 to 2014, the optimal orientation for station PHRA was −150°, indicating that the North component was almost oriented to the south. After 2014, the N-S orientation of this station was changed to 10° (Table 1), probably as a result of manual adjustment.

3.2. Crustal thickness and V_p/V_s observations

A total of 13,940 high-quality RFs were used for conducting H-κ stacking in this study. The number of RFs per station ranges from 37 to 4774 with a simple mean of 435. The resulting crustal thickness ranged from 27.1 km along the coast to 40.7 km inside the Indochina Block with an average value of 32.1±3 km, and the V_p/V_s varied from 1.65 to 1.91 with a simple mean of 1.76 ± 0.07 (Fig. 4 and Table 1). The mean H and κ are comparable with the global averages of 34 km and 1.78 for continental crust (Zandt and Ammon, 1995; Christensen, 1996).

The distribution of H and κ is closely associated with the tectonic background. Stations located in the coastal area of the Indochina Peninsula are generally characterized by a thinner-than-normal crust of less than 30 km thick with spatially varying κ, which is consistent with a previous RF study in Thailand (Noisagool et al., 2014). Among the 32 stations, 5 were situated within the southern part of the Shan Thai Block and were found to have an average H of 31.4±1.2 km and a mean κ value of 1.75 ± 0.05.

Based on the characteristics of the resulting κ values, the Indochina Block can be divided into southern and northern parts. The

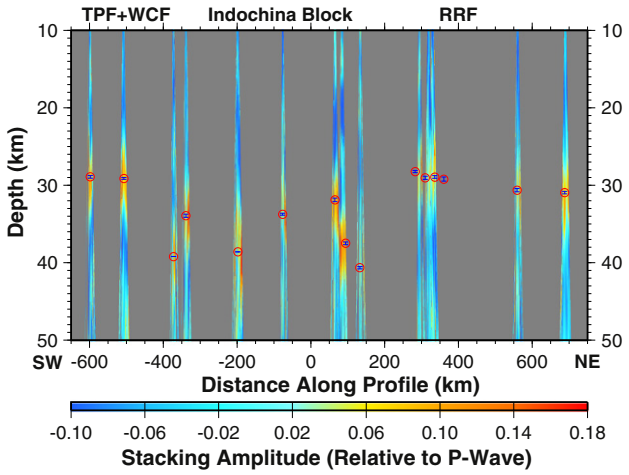

Fig. 3. Profile of normal moveout migrated RFs from stations within the black rectangle along the black dashed line in Fig. 1. The red circles with blue error bars indicate results from H-κ stacking. (For interpretation of the references to color in this figure legend, the reader is referred to the web version of this article.)

northern part is generally composed of the Khorat Plateau (Fig. 1) and has an average crustal H and κ of 36.9±3 km and 1.74±0.04, respectively (Fig. 4 and Table 1). In comparison, the southern part displays a relatively thinner crust (31.3 ± 2.9 km) and higher κ (1.83 ± 0.03). The κ values within the deformation zone between the Red River Fault and Song Ma Suture are mostly higher than 1.8, while the surrounding areas are highlighted by smaller κ measurements of 1.75 or less.

In order to maximize the spatial coverage of crustal H-κ measurements, in Fig. 4 and in the discussions below, we also included results ranked as quality A from previous studies at stations from which data are unavailable to us (Nguyen et al., 2013; Noisagool et al., 2014). Both Fig. 4 and Table 1 show that our observations in the same regions are in general agreement with previous RF studies (Bai et al., 2010; Nguyen et al., 2013; Noisagool et al., 2014).

4. Discussion

Laboratory experiments show that the κ value of common crustal rocks varies from 1.63 to 2.08 (Holbrook et al., 1992). In general, the κ value for felsic rocks is lower than 1.76; it is between 1.76 and 1.81 for intermediate rocks, and above 1.81 for mafic rocks (Holbrook et al., 1992). Based on these criteria, we estimated the general crustal compositions of different tectonic domains and speculate on the causes leading to the spatial variations of the observed crustal properties. In addition to mafic crustal composition, partial melting can also significantly increase the κ of crustal rocks. For instance, Watanabe (1993) found that κ increases as a continuous function of the melt fraction of felsic rocks, mostly due to a more rapid reduction of V_s relative to V_p. Such melt-induced increase in κ has been used to explain anomalously large κ values obtained in areas with pervasive Cenozoic volcanisms including the Afar Depression (Reed et al., 2014) and northeastern Japan (Nakajima et al., 2001). It can also be responsible for the high κ measurements observed along major faults in the study area, and in the volcanic southern Indochina Block (Fig. 4b), as detailed below.

4.1. Contrasting crustal properties across the Red River Fault

The Red River Fault is commonly considered to be a lithospheric-scale strike slip fault that has accommodated at least 500 kilometers of the southeastward extrusion of the Indochina Peninsula resulted

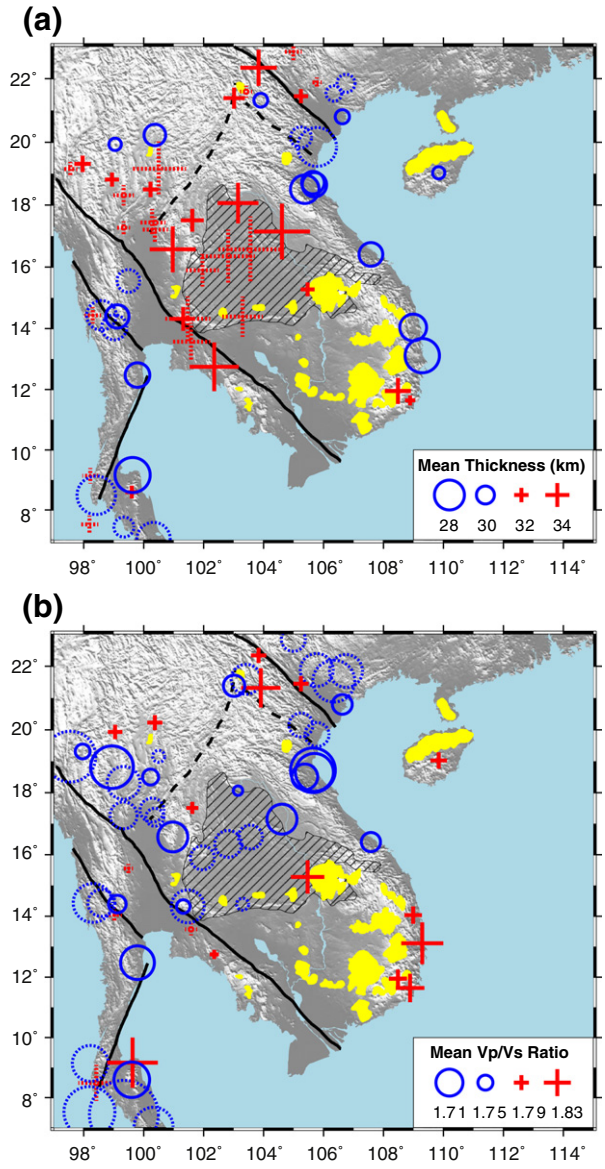

Fig. 4. Resulting crustal thickness and V_p/V_s measurements. Pluses and open circles indicate larger and smaller values, respectively (see legend). Dashed pluses and circles show results from previous studies (Nguyen et al., 2013; Noisagool et al., 2014). The area filled with slashed lines is the Khorat Basin, and the yellow shaded areas are Cenozoic volcanic centers. (For interpretation of the references to color in this figure legend, the reader is referred to the web version of this article.)

from the indentation of the Indian into Eurasian plates (e.g., Yang and Besse, 1993; Leloup et al., 1995; Chung et al., 1997; Charusiri et al., 2006; Huang et al., 2013; Legendre et al., 2015). Seismic tomography studies proposed that the Red River Fault probably has cut through the crust and reached up to the upper mantle (Wu et al., 2004; Huang et al., 2013, 2015), a conclusion that is consistent with the contrasting crustal properties across the fault from the current and previous RF studies (Xu et al., 2006; Nguyen et al., 2013).

Areas to the northeast of the Red River Fault have a felsic crustal composition similar to that of the stable South China Block (Nguyen et al., 2013). In contrast, the higher κ values (>1.81) within the deformation zone between the Red River Fault and the Song Ma Suture may imply a mafic crustal composition. Both body and surface wave tomography studies proposed that low velocity anomalies exist in the lower crust and uppermost mantle beneath this deformation zone (e.g., Xu et al., 2005; Huang et al., 2013, 2015). The localization

of lithospheric deformation along the Red River Fault (Yang et al., 2015) resulted from relative motions between the South China and Indochina Blocks possibly induced the intrusion of hot mafic mantle materials into the crust, leading to the observed high κ values.

4.2. Preservation of ancient crust beneath the Indochina Block

The Indochina Block is believed to have a rigid continental root, experiencing much less internal deformation relative to the surrounding regions (e.g., Charusiri et al., 2006; Sato et al., 2007; Takemoto, 2009; Yang et al., 2015; Tsuchiyama et al., 2016). The Khorat Plateau, which occupies the core of the Indochina Block, is characterized by small κ (1.74 ± 0.04) and large H (36.9 ± 3 km) values, which are similar to those observed on stable regions of the South China Block such as the Sichuan Basin east of the Tibetan Plateau (e.g., Chen et al., 2010). Such a similarity suggest that the central part of the Indochina Block may represent the original crust of the Indochina Peninsula before the extrusion, and that the lithosphere of the Plateau has suffered insignificant deformation.

4.3. Crustal modification beneath the Southern Indochina Block

The volcanic southern portion of the Indochina Block is underlain by a more mafic crust, probably the result of basaltic intrusion that has been investigated intensively by previous studies (Rangin et al., 1995; Hoang and Flower, 1998; Noisagool et al., 2014). The mafic rocks in this area may be associated with the Mesozoic subduction (e.g., Hall, 2002; Morley, 2012; Tang and Zheng, 2013), although such a model is difficult to explain the fact that some of the volcanoes are currently active.

Another possibility is that the mafic crustal rocks in this area are the result of mantle upwelling in response to the thinned lithosphere. Early investigations of basalt magmatism in Vietnam indicated that the collision-induced extrusion promoted the thinning of the lithosphere, resulting in penetration and advanced polybaric melting of the low viscosity upper mantle (Hoang and Flower, 1998). In addition, low seismic velocity anomalies have been identified within the lithosphere in this area (e.g., Huang et al., 2015; Yang et al., 2015; Tsuchiyama et al., 2016), implying a warmer and possibly partially-melted lithosphere beneath the southern part of the Indochina Block.

5. Conclusions

Our observations combined with results from previous studies show that indentation-induced clockwise rotation and southward movement of the Indochina Peninsula relative to Eurasia resulted in spatially heterogeneous internal deformations in the Indochina Peninsula. Areas along major strike-slip faults as well as areas with thinned lithosphere are found to possess an overall mafic crust, while the core of the Indochina Block has a thick and felsic crust that is similar in nature to undeformed regions in the South China Block. The significant heterogeneity in the lateral distribution of crustal properties and its correspondence with indentation-related tectonic features such as strike-slip faults and thinned lithosphere, are more consistent with block extrusion than viscous type models for lithospheric deformation of the Indochina Peninsula.

Acknowledgments

We thank the Earthquake Research Institute of the University of Tokyo for sharing the Vietnam array data, which can be accessed by filing a request to breq-fast-vietnet@ohpdmc.eri.u-tokyo.ac.jp. We also thank the IRIS DMC for archiving the data from the permanent stations used in this study. Data from the 6 stations of the temporary network in Vietnam are collected and archived by the seismology groups in Tongji University and Hanoi University of Mining and Geology. Constructive comments from two anonymous reviewers significantly improved the manuscript. This study is funded by the National Natural Science Foundation of China through grants 41606043 and 41676033, and the National Program on Global Change and Air-Sea Interaction under grant GASI-GEOGE-05.

References

Achache, J., Courtillot, V., Besse, J., 1983. Paleomagnetic constraints on the late Cretaceous and Cenozoic tectonics of southeastern Asia. Earth Planet. Sci. Lett. 63 (1), 123–136. http://dx.doi.org/10.1016/0012-821X(83)90028-6.

Ammon, C.J., 1991. The isolation of receiver effects from teleseismic *P*-waveforms. Bull. Seismol. Soc. Am. 81, 2504–2510.

Bai, L., Iidaka, T., Kawakatsu, H., Morita, Y., Dzung, N.Q., 2009. Upper mantle anisotropy beneath Indochina Block and adjacent regions from shear-wave splitting analysis of Vietnam broadband seismograph array data. Phys. Earth Planet. Inter. 176 (1), 33–43. http://dx.doi.org/10.1016/j.pepi.2009.03.008.

Bai, L., Tian, X., Ritsema, J., 2010. Crustal structure beneath the Indochina Peninsula from teleseismic receiver functions. Geophys. Res. Lett. 37, L24308. http://dx.doi.org/10.1029/2010GL044874.

Briais, A., Patriat, P., Tapponnier, P., 1993. Updated interpretation of magnetic anomalies and seafloor spreading stages in the South China Sea: implications for the Tertiary tectonics of Southeast Asia. J. Geophys. Res. 98 (B4), 6299–6328. http://dx.doi.org/10.1029/92JB02280.

Charusiri, P., Imsamut, S., Zhuang, Z., Ampaiwan, T., Xu, X., 2006. Paleomagnetism of the earliest Cretaceous to early late Cretaceous sandstones, Khorat Group, Northeast Thailand: implications for tectonic plate movement of the Indochina Block. Gondwana Res. 9 (3), 310–325. http://dx.doi.org/10.1016/j.gr.2005.11.006.

Chen, Y., Niu, F., Liu, R., Huang, Z., Tkalcic, H., Sun, L., Chan, W., 2010. Crustal structure beneath China from receiver function analysis. J. Geophys. Res. 115, B03307. http://dx.doi.org/10.1029/2009JB006386.

Chi, C.T., Geissman, J.W., 2013. A review of the paleomagnetic data from Cretaceous to lower Tertiary rocks from Vietnam, Indochina and South China, and their implications for Cenozoic tectonism in Vietnam and adjacent areas. J. Geodyn. 69, 54–64. http://dx.doi.org/10.1016/j.jog.2011.11.008.

Christensen, N.I., 1996. Poisson's ratio and crustal seismology. J. Geophys. Res. 101 (B2), 3139–3156. http://dx.doi.org/10.1029/95JB03446.

Chung, S.L., Lee, T.Y., Lo, C.H., Wang, P.L., Chen, C.Y., Yem, N.T., Hoa, T.T., Genyao, W., 1997. Intraplate extension prior to continental extrusion along the Ailao Shan-Red River shear zone. Geology 25 (4), 311–314. http://dx.doi.org/10.1130/0091-7613(1997)025<0311:IEPTCE>2.3.CO;2.

Efron, B., Tibshirani, R., 1986. Bootstrap methods for standard errors, confidence intervals, and other measures of statistical accuracy. Stat. Sci. 1, 54–75.

England, P., Houseman, G., 1986. Finite strain calculations of continental deformation: 2. Comparison with the India-Asia collision zone. J. Geophys. Res. 91 (B3), 3664–3676. http://dx.doi.org/10.1029/JB091iB03p03664.

Fedorov, P.I., Koloskov, A.V., 2005. Cenozoic volcanism of Southeast Asia. Petrology 13, 352–380.

Hall, R., 2002. Cenozoic geological and plate tectonic evolution of SE Asia and the SW Pacific: computer-based reconstructions, model and animations. J. Asian Earth Sci. 20 (4), 353–431. http://dx.doi.org/10.1016/S1367-9120(01)00069-4.

Hoang, N., Flower, M., 1998. Petrogenesis of Cenozoic basalts from Vietnam: implications for origin of a 'diffuse igneous province'. J. Petrol. 39, 369–395. http://dx.doi.org/10.1093/petroj/39.3.369.

Holbrook, W.S., Mooney, W.D., Christensen, N.I., 1992. The Seismic Velocity Structure of the Deep Continental Crust, in Continental Lower Crust. In: Fountain, D.M., Arculus, R., Kay, W. (Eds.), Elsevier, New York, pp. 21–43.

Huang, H.H., Xu, Z.J., Wu, Y.M., Song, X., Huang, B.S., Nguyen, L.M., 2013. First local seismic tomography for Red River shear zone, northern Vietnam: stepwise inversion employing crustal P and Pn waves. Tectonophysics 584, 230–239. http://dx.doi.org/10.1016/j.tecto.2012.03.030.

Huang, Z., Zhao, D., Wang, L., 2015. *P* wave tomography and anisotropy beneath Southeast Asia: insight into mantle dynamics. J. Geophys. Res. 120, 5154–5174. http://dx.doi.org/10.1002/2015JB012098.

Huchon, P., Le Pichon, X., Rangin, C., 1994. Indochina Peninsula and the collision of India and Eurasia. Geology 22, 27–30. http://dx.doi.org/10.1130/0091-7613(1994)022<0027:IPATCO>2.3.CO;2.

Langston, C.A., 1979. Structure under Mount Rainier, Washington, inferred from teleseismic body waves. J. Geophys. Res. 84, 4749–4762. http://dx.doi.org/10.1029/JB084iB09p04749.

Legendre, C.P., Zhao, L., Huang, W.G., Huang, B.S., 2015. Anisotropic Rayleigh-wave phase velocities beneath northern Vietnam. Earth Planets Space 67, 28. http://dx.doi.org/10.1186/s40623-015-0193-3.

Leloup, P.H., Lacassin, R., Tapponnier, P., Scharer, U., Zhong, D., Liu, X., Zhang, L., Ji, S., Trinh, P.T., 1995. The Ailao Shan-Red River shear zone (Yunnan, China), Tertiary transform boundary of Indochina. Tectonophysics 251 (1), 3–84. http://dx.doi.org/10.1016/0040-1951(95)00070-4.

Liu, K.H., Gao, S.S., 2010. Spatial variations of crustal characteristics beneath the Hoggar swell, Algeria, revealed by systematic analyses of receiver functions from a single seismic station. Geochem. Geophys. Geosyst. 11, Q08011. http://dx.doi.org/10.1029/2010GC003091.

Morley, C.K., 2012. Late Cretaceous-Early Paleogene tectonic development of SE Asia,. Earth Sci. Rev. 115, 37–75. http://dx.doi.org/10.1016/j.earscirev.2012.08.002.
Nakajima, J., Matsuzawa, T., Hasegawa, A., Zhao, D., 2001. Three-dimensional structure of Vp, Vs, and Vp/Vs beneath northeastern Japan: implications for arc magmatism and fluids. J. Geophys. Res. 106 (B10), 21843–21857. http://dx.doi.org/10.1029/2000JB000008.
Nguyen, V.D., Huang, B.S., Le, T.S., Dinh, V.T., Zhu, L., Wen, K., 2013. Constraints on the crustal structure of northern Vietnam based on analysis of teleseismic converted waves. Tectonophysics 601, 87–97. http://dx.doi.org/10.1016/j.tecto.2013.04.031.
Niu, F., Li, J., 2011. Component azimuths of the CEArray stations estimated from *P*-wave particle motion. Earthq. Sci. 24, 3–13. http://dx.doi.org/10.1007/s11589-011-0764-8.
Noisagool, S., Boonchaisuk, S., Pornsopin, P., Siripunvaraporn, W., 2014. Thailand's crustal properties from tele-seismic receiver function studies. Tectonophysics 632, 64–75. http://dx.doi.org/10.1016/j.tecto.2014.06.014.
Otofuji, Y.I., Tung, V.D., Fujihara, M., Tanaka, M., Yokoyama, M., Kitada, K., Zaman, H., 2012. Tectonic deformation of the southeastern tip of the Indochina Peninsula during its southward displacement in the Cenozoic time. Gondwana Res. 22, 615–627. http://dx.doi.org/10.1016/j.gr.2011.09.015.
Rangin, C., Huchon, P., Le Pichon, X., Bellon, H., Lepvrier, C., Roques, D., Hoe, N.D., Quynh, P.V., 1995. Cenozoic deformation of central and south Vietnam. Tectonophysics 251, 179–196. http://dx.doi.org/10.1016/0040-1951(95)00006-2.
Reed, C.A., Almadani, S., Gao, S.S., Elsheikh, A.A., Cherie, S., Abdelsalam, M.G., Thurmond, A.K., Liu, K.H., 2014. Receiver function constraints on crustal seismic velocities and partial melting beneath the Red Sea rift and adjacent regions, Afar Depression. J. Geophys. Res. Solid Earth 119, 2138–2152. http://dx.doi.org/10.1002/2013JB010719.
Richter, B., Fuller, M., Blundell, E., 1996. Palaeomagnetism of the Sibumasu and Indochina blocks: implications for the extrusion tectonic model. In: Hall, R. (Ed.), Tectonic Evolution for Southeast Asia, Geol. Soc. Spec. Publ., 106(1). pp. 203–224. http://dx.doi.org/10.1144/GSL.SP.1996.106.01.13.
Sato, K., Liu, Y., Wang, Y., Yokoyama, M., Yoshioka, S.Y., Yang, Z., Otofuji, Y.I., 2007. Paleomagnetic study of Cretaceous rocks from Pu'er, western Yunnan, China: evidence of internal deformation of the Indochina Block. Earth Planet. Sci. Lett. 258 (1), 1–15. http://dx.doi.org/10.1016/j.epsl.2007.02.043.
Sato, K., Liu, Y., Zhu, Z., Yang, Z., Otofuji, Y.I., 2001. Tertiary paleomagnetic data from northwestern Yunnan, China: further evidence for large clockwise rotation of the Indochina Block and its tectonic implications. Earth Planet. Sci. Lett. 185 (1), 185–198. http://dx.doi.org/10.1016/S0012-821X(00)00377-0.
Searle, M.P., 2006. Role of the Red River shear zone, Yunnan and Vietnam, in the continental extrusion of SE Asia. J. Geol. Soc. 163 (6), 1025–1036. http://dx.doi.org/10.1144/0016-76492005-144.
Tadapansawut, T., Chaisri, S., Naunnin, P., 2012. Thailand crustal thickness estimate using joint inversion of surface wave dispersion and receiver function. The 6th International Conference on Applied Geophysics. Kanchanaburi.,
Takemoto, K., et al. 2009. Tectonic deformation of the Indochina Peninsula recorded in the mesozoic palaeomagnetic results. Geophys. J. Int. 179 (1), 97–111. http://dx.doi.org/10.1111/j.1365-246x.2009.04274.x.
Tang, Q., Zheng, C., 2013. Crust and upper mantle structure and its tectonic implications in the South China Sea and adjacent regions. J. Asian Earth Sci. 62, 510–525. http://dx.doi.org/10.1016/j.jseaes.2012.10.037.
Tapponnier, P., Peltzer, G., Le Dain, A.Y., Armijo, R., Cobbold, P., 1982. Propagating extrusion tectonics in Asia: new insights from simple experiments with plasticine. Geology 10, 611–616. http://dx.doi.org/10.1130/0091-7613(1982)10<611:PETIAN>2.0.CO;2.
Tsuchiyama, Y., Zamanb, H., Sothamc, S., Samuthc, Y., Satod, E., Ahna, H.S., Unoe, K., Tsumuraa, K., Mikia, M., Otofujia, Y.I., 2016. Paleomagnetism of Late Jurassic to Early Cretaceous red beds from the Cardamom Mountains, southwestern Cambodia: tectonic deformation of the Indochina Peninsula. Earth Planet Sci. Lett. 434, 274–288. http://dx.doi.org/10.1016/j.epsl.2015.11.045.
Watanabe, T., 1993. Effects of water and melt on seismic velocities and their application to characterization of seismic reflectors. Geophys. Res. Lett. 20, 2933–2936.
Wen, S., Yeh, Y.L., Tang, C.C., Phong, L.H., Toan, D.V., Chang, W.Y., Chen, C.H., 2015. The tectonic structure of the Song Ma fault zone, Vietnam. J. Asian Earth Sci. 107, 26–34. http://dx.doi.org/10.1016/j.jseaes.2015.03.046.
Wu, H.H., Tsai, Y.B., Lee, T.Y., Lo, C.H., Hsieh, C.H., Toan, D.V., 2004. 3-D shear wave velocity structure of the crust and upper mantle in South China Sea and its surrounding regions by surface wave dispersion analysis. Mar. Geophys. Res. 25, 5–27. http://dx.doi.org/10.1007/s11001-005-0730-8.
Xu, M., Wang, L., Liu, J., Zhong, K., Li, H., Hu, D., Xu, Z., 2006. Crust and uppermost mantle structure of the Ailaoshan-Red River fault from receiver function analysis. Sci. China Ser. D 49 (10), 1043–1052. http://dx.doi.org/10.1007/s11430-006-1043-8.
Xu, Y., Liu, J., Liu, F., Song, H., Hao, T., Jiang, W., 2005. Crust and upper mantle structure of the Ailao Shan-Red River fault zone and adjacent regions. Sci. China Ser. D 48 (2), 156–164. http://dx.doi.org/10.1360/02yd0386.
Yang, T., Liu, F., Harmon, N., Le, K.P., Gu, S., Xue, M., 2015. Lithospheric structure beneath Indochina Block from Rayleigh wave phase velocity tomography. Geophys. J. Int. 200 (3), 1582–1595. http://dx.doi.org/10.1093/gji/ggu488.
Yang, Z., Besse, J., 1993. Paleomagnetic study of Permian and Mesozoic sedimentary rocks from Northern Thailand supports the extrusion model for Indochina. Earth Planet. Sci. Lett. 117 (3), 525–552. http://dx.doi.org/10.1016/0012-821X(93)90101-E.
Yu, Y., Song, J., Liu, K.H., Gao, S.S., 2015a. Determining crustal structure beneath seismic stations overlying a low-velocity sedimentary layer using receiver functions. J. Geophys. Res. 120, 3208–3218. http://dx.doi.org/10.1002/2014JB011610.
Yu, Y., Liu, K.H., Reed, C.A., Moidaki, M., Mickus, K., Atekwana, E.A., Gao, S.S., 2015b. A joint receiver function and gravity study of crustal structure beneath the incipient Okavango Rift, Botswana. Geophys. Res. Lett. 42, 8398–8405. http://dx.doi.org/10.1002/2015GL065811.
Zandt, G., Ammon, C.J., 1995. Continental crust composition constrained by measurements of crustal Poisson's ratio. Nature 374, 152–154. http://dx.doi.org/10.1038/374152a0.
Zhu, L., Kanamori, H., 2000. Moho depth variation in southern California from teleseismic receiver functions. J. Geophys. Res. 105 (B2), 2969–2980. http://dx.doi.org/10.1029/1999JB900322.